# Supporting information

## Nanotube array-based barium titanate-cobalt ferrite composite film for affordable magnetoelectric multiferroics

Go Kawamura,*[ab] Kentaro Oura,[a] Wai Kian Tan,[c] Taichi Goto,[ad] Yuichi Nakamura,[a] Daisaku Yokoe,[e] Francis Leonard Deepak,[f] Khalil El Hajraoui,[f] Xing Wei,[g] Mitsuteru Inoue,[a] Hiroyuki Muto,[c] Kazuhiro Yamaguchi,[h] Aldo R. Boccaccini[b] and Atsunori Matsuda[a]

[a]Department of Electrical and Electronic Information Engineering, Toyohashi University of Technology, 1-1 Hibarigaoka, Tempaku-cho, Toyohashi, 441-8580 Aichi, Japan. E-mail: gokawamura@ee.tut.ac.jp

[b]Institute of Biomaterials, University of Erlangen-Nuremberg, Germany

[c]Institute of Liberal Arts and Science, Toyohashi University of Technology, Japan

[d]JST, PRESTO, Japan

[e]Nanostructures Research Laboratory, Japan Fine Ceramics Center, Japan

[f]Nanostructured Material Group, Department of Advanced Electron Microscopy, Image and Spectroscopy, International Iberian Nanotechnology Laboratory, Portugal

[g]School of Materials Science and Engineering, Chang'an University, China

[h]Electrical and Electronic Engineering Course, National Institute of Technology, Ibaraki College, Japan

*Correspondence: gokawamura@ee.tut.ac.jp (G.K.)

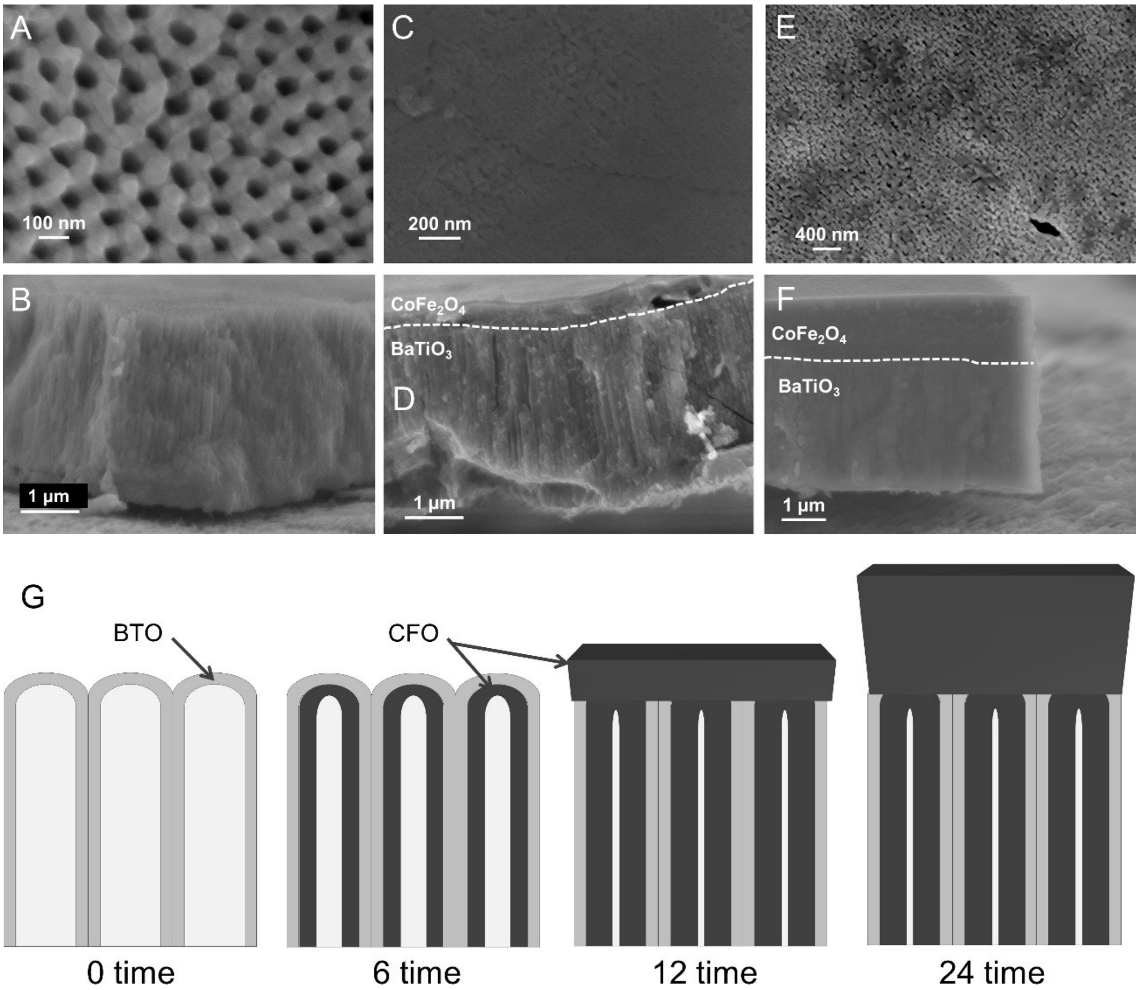


**Fig. S1** SEM images of BTO-CFO nanocomposite films prepared by 6-time (A, B), 12-time (C, D), and 24-time spin coatings (E, F). A pure CFO layer was observed on the top of the nanotube arrays when the coating number was 12 times or more, though the tubular pores of BTO NTs were not completely filled with CFO. (G) is a schematic illustration to describe the progress of CFO deposition.

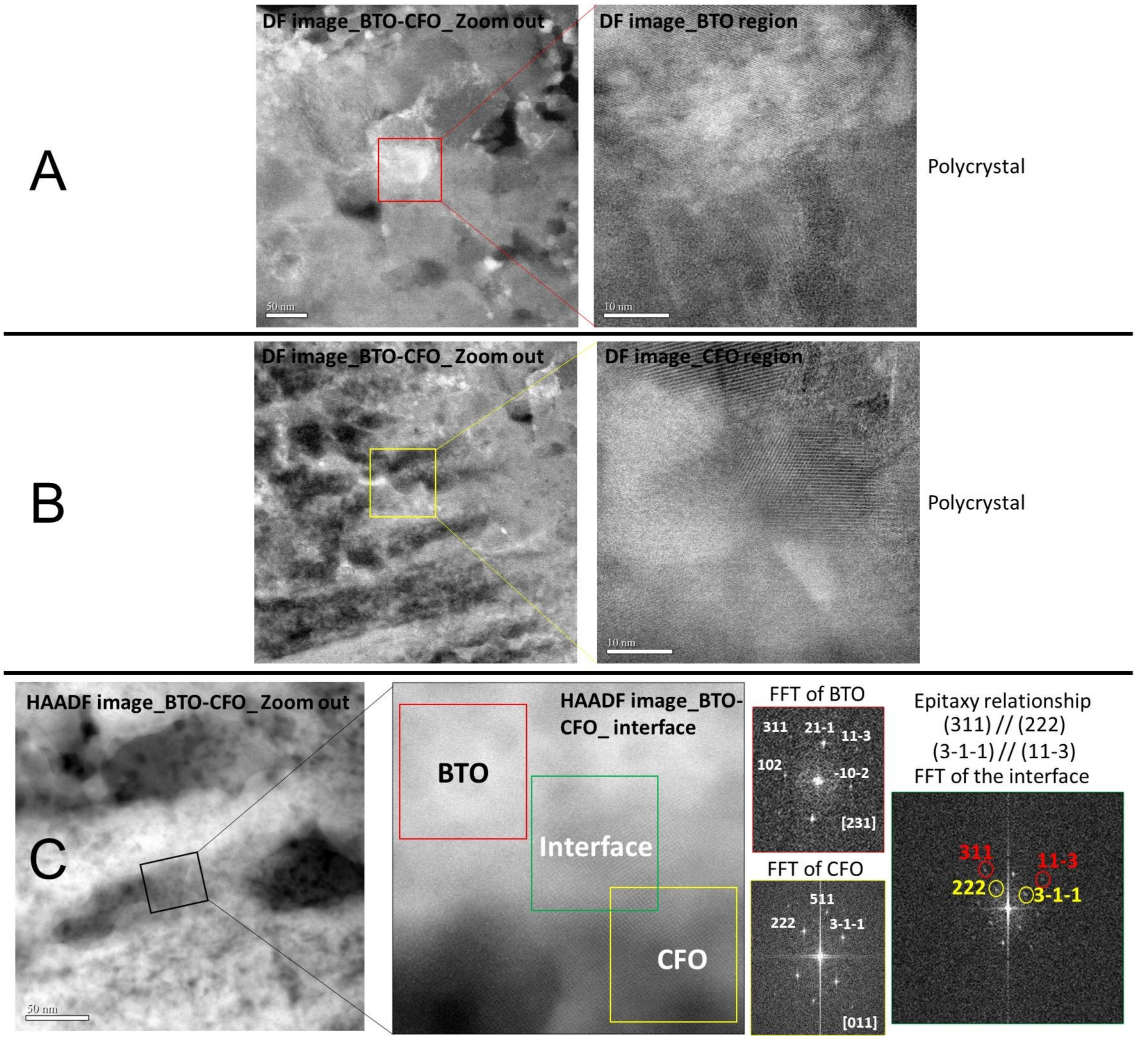


**Fig. S2** Dark field (DF) images at the BTO (A) and CFO (B) regions in the BTO-CFO nanocomposite film. HAADF-STEM images and the corresponding fast fourier transformation (FFT) at the interface region of BTO and CFO in the BTO-CFO nanocomposite film (C). The BTO and CFO are basically polycrystals, which are proved by a perfect match between their XRD patterns (Fig. 2) and the powder XRD data (JCPDS 05-626 (BTO) and 22-1086 (CFO)), but they have epitaxy relationship at their interface region. The epitaxy relationship of BTO and CFO would contribute to a large magnetoelectric effect in the nanocomposite film due to seamless strain transfer.

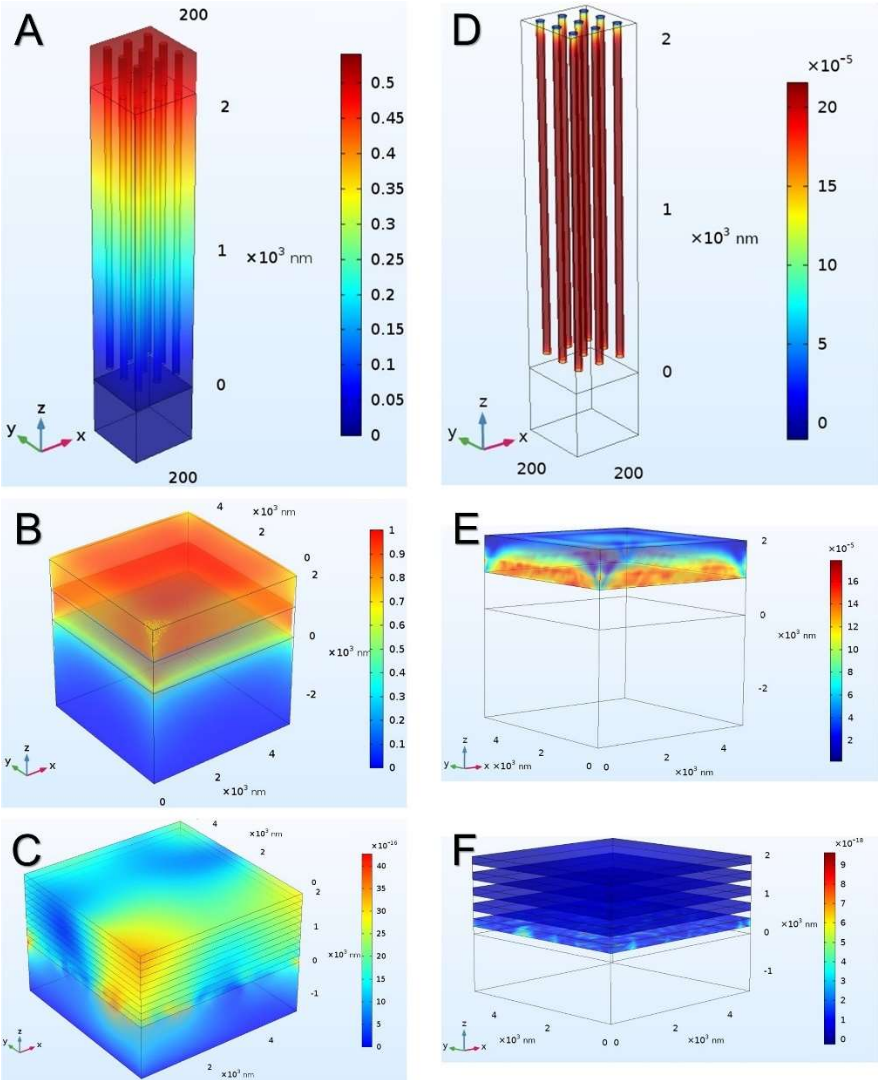


**Fig. S3** Finite element (COMSOL) simulations of deformation of nanocomposite film (A, B and C) and distortion distribution in CFO components (D, E and F). The modeling details are as follows: (A and D) The radius and length of CFO cylindrical nanopillars are 25 and 2000 nm, respectively. The periodicity of the pillars is 150 nm. The other part of the composite (matrix) is BTO; (B and E) 1000 nm CFO film was on 1000 nm BTO film; (C and F) 200 nm CFO and 200 nm BTO films are accumulated alternatively to form multilayer structure. For all models, the substrate material is Ti. The electric potential of 5 V is applied on the top surface of the composite film, and the bottom of the film is set to be ground. The largest deformation is observed in the bilayer sample. On the other hand, the largest distortion is observed in the nanopillar array-based sample, and almost whole part in CFO nanopillars is largely distorted in the sample. The large distortion in CFO, which results from efficient strain transfer form BTO to CFO, leads to large ME effect.

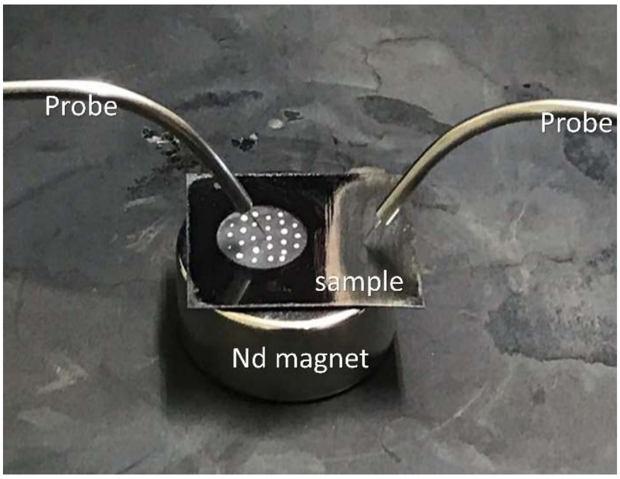


**Fig. S4** Photograph taken during the magnetoelectric effect measurement. The dielectric property was measured using non-magnetic probes. The probes were attached to the Ti substrate as a bottom electrode and Ag paste applied on the nanocomposite film surface as a top electrode. A Nd magnet (surface magnetic flux density: 350 mT) was placed under the sample to apply an external magnetic field.

**Table S1** EDX results of BTO-CFO nanocomposite

| | Surface | Cross-sec. (top) | Cross-sec. (bottom) |
|---|---|---|---|
| Ba | 14.7 | 9.3 | 10.3 |
| Ti | 12.5 | 8.8 | 19.2 |
| Co | 4.9 | 1.9 | 2.8 |
| Fe | 9.5 | 4.5 | 4.9 |
| O | 54.2 | 66.9 | 59.2 |

**Table S2** Coercivity and remnant magnetization values

| Sample | Configuration | Coercivity (mT) | Remnant Magnetization, $M_r$ (emu $cm^{-3}$) |
|---|---|---|---|
| Pure CFO | in-plane | 1.57 | 164 |
| | out-of-plane | 1.33 | 127 |
| BTO-CFO | in-plane | 1.40 | 193 |
| | out-of-plane | 1.40 | 199 |